Small binding-site clearance delays are not negligible in gene expression modeling

Elizabeth A. M. Trofimenkoff, Marc R. Roussel*

Alberta RNA Research and Training Institute, Department of Chemistry and Biochemistry, University of Lethbridge, Lethbridge, Alberta, Canada, T1K 3M4

Abstract

During the templated biopolymerization processes of transcription and translation, a macromolecular machine, either an RNA polymerase or a ribosome, binds to a specific site on the template. Due to the sizes of these enzymes, there is a waiting time before one clears the binding site and another can bind. These clearance delays are relatively short, and one might think that they could be neglected. However, in the case of transcription, these clearance delays are associated with conservation laws, resulting in surprisingly large effects on the bifurcation diagrams in models of gene expression networks. We study an example of this phenomenon in a model of a gene regulated by a non-coding RNA displaying bistability. Neglecting the binding-site clearance delays in this model can only be compensated for by making ad hoc, unphysical adjustments to the model's kinetic constants.

Keywords: Gene expression modeling, delays, binding-site clearance, processive enzymes

1. Introduction

A macromolecular machine such as an RNA polymerase or a ribosome that binds to a nucleic acid polymer (DNA or RNA) excludes other machines from

---

*Corresponding author
Email addresses:* `elizabeth.pedersen@uleth.ca` (Elizabeth A. M. Trofimenkoff), `roussel@uleth.ca` (Marc R. Roussel)

accessing the nucleotides to which the machine is bound. This observation is the basis for Totally Asymmetric Exclusion Process (TASEP) and related models of transcription and translation [1–6]. In particular, the binding of one of these machines to initiate a biopolymerization process occludes the binding site, which must be cleared before another machine can bind. These effects can be incorporated in a simple way into gene expression models by including a binding-site clearance delay into the initiation process [7], or by modeling clearance explicitly [8–12].

In many mathematical models involving delays, the steady states do not depend on the delays because, in a steady state, $x(t - \tau) = x(t)$. In particular, the number and coordinates of the steady states might be thought to be properties that do not depend on whether or not delays are considered. Absent other types of bifurcations, this line of reasoning would lead us to conclude that bistability is a phenomenon that is independent of the delays. However, there is one important case in which the steady states *do* depend on the delays, and that is the case in which a conserved component of the system enters a process from which it only exits with a delay. Gene promoter clearance is an example of this: transcription initiation occludes the promoter, which only becomes available again once the transcription machinery has cleared the promoter (Fig 1). In cells that are not actively replicating, the total amount of a given promoter in a cell is fixed by the cell's ploidy. In sufficiently slowly replicating cells, it may still be a good approximation to treat the promoter concentration as fixed, at least outside of the DNA synthesis phase of the cell cycle. Conserved quantities like the promoter concentration that are recycled with a delay lead to integral conservation relationships that depend on the size of the delay [14]. For binding sites (gene promoters, ribosome binding sites), this can have the effect of reducing the amount of free binding site available at any given time, with potential effects (depending on the structure of the model) on the steady state values of other variables [15]. Quite apart from the importance of these effects in mathematical modeling, these are real biological phenomena that have also been studied experimentally [16–19].
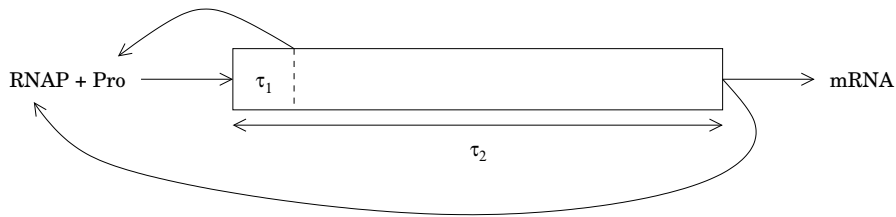
2

Figure 1: Delays in transcription: The RNA polymerase (RNAP) and promoter form a complex. A time τ_1 elapses before the polymerase clears the promoter and the latter is once again available for transcription initiation. Completion of the transcript requires a total time τ_2. Neglecting the difference in time between completion of the transcript and release of the polymerase, which are not necessarily simultaneous events [13], RNAP is also recycled after τ_2. Because many transcripts are simultaneously transcribed by many polymerases, there is no specific pool of polymerases associated with one particular transcript, so that the initiation or termination of transcription will normally have a negligible effect on the the cellular RNAP pool, hence our treatment of this pool as being fixed.

For transcription in particular, in prokaryotes, measured mean promoter clearance times vary from 4 s to 40 min [11, 20–22]. In eukaryotes, the mean promoter clearance time is of the order of 8 to 10 minutes [23, 24]. With rare exceptions [7, 15, 25, 26], these clearance delays, which are short compared to the time required to produce a mature transcript, are ignored in gene expression models, although they are automatically included in any nucleotide-resolution transcription or translation model [10, 26–28]. Given that these delays are relatively short, they might be thought to be negligible. The effects of clearance delays in a bistable model for NO detoxification in bacteria were briefly mentioned in a recent study [15]. On further study of this model, one of us found that there were relatively large changes in the bifurcation diagram of the model depending on whether or not binding-site clearance delays were included (E. A. M. Trofimenkoff, unpublished). One simple idea we pursued was that the differences between models with and without delays might be due to differences in the initiation frequencies of transcription and translation, since occlusion of the binding site necessarily increases the mean time between initiations. Attempts to compensate for the absence of delays on this basis did not eliminate

the differences in the bifurcation diagrams, and in fact sometimes made them worse.

The NO detoxification model is relatively complex, and so is not a good platform for deeper analysis. We therefore chose to examine the effects of binding-site clearance delays in a mass-action elaboration of a model with bistable behavior due to the control of translation through a non-coding RNA (ncRNA) proposed by Zhdanov [29]. From the point of view of our current study, this model has several attractive features beyond its relative simplicity. It includes transcription and translation, both of which are subject to binding-site clearance effects. The mRNA is expressed constitutively, while expression of the ncRNA is repressed by the protein encoded by the mRNA. This allows us to consider the effects of binding-site clearance delays in both regulated and unregulated transcription processes. Similar models with transcription and translation delays have appeared elsewhere, and could also have formed the basis for this study [30, 31].

In Sect. 2, we construct a delayed mass-action model [14] corresponding to Zhdanov's model, and derive the steady-state conditions for this model both with and without delays. In Sect. 3, we show that this model has a bistable regime, both analytically and numerically. In particular, we calculate some bifurcation curves for the models with and without delays to demonstrate the non-negligible effects of the clearance delays. In Sect. 4, we obtain parameter transformations that will bring the two models into correspondence. We point out that these transformations require unphysical adjustments to the kinetic parameters. Finally, we discuss the implications of this work both for predictive modeling and for model fitting.
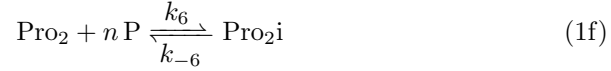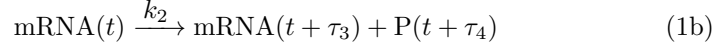
2. The elaborated Zhdanov model

2.1. The model with delays

Zhdanov's original model included an empirical functional form for the transcription rate of the non-coding RNA assuming independent binding of n units

of the protein to the promoter [29]. For this study, we needed to explicitly consider the state of the promoter. We thus replaced Zhdanov's empirical rate law by cooperative binding of n proteins to the promoter. While this yields slightly different kinetics, it has the benefit of not adding many chemical reaction steps while allowing for the explicit representation of events at the promoter needed here.

The model we studied is the following, expressed in the delayed mass-action notation [14], with the time index (t) being suppressed in reactions containing no delayed terms:

$$\text{Pro}_1(t) \xrightarrow{k_1} \text{Pro}_1(t + \tau_1) + \text{mRNA}(t + \tau_2) \tag{1a}$$

$$\text{mRNA}(t) \xrightarrow{k_2} \text{mRNA}(t + \tau_3) + \text{P}(t + \tau_4) \tag{1b}$$

$$\text{mRNA} \xrightarrow{k_3} \emptyset \tag{1c}$$

$$\text{P} \xrightarrow{k_4} \emptyset \tag{1d}$$

$$\text{Pro}_2(t) \xrightarrow{k_5} \text{Pro}_2(t + \tau_5) + \text{ncRNA}(t + \tau_6) \tag{1e}$$

$$\text{Pro}_2 + n\,\text{P} \underset{k_{-6}}{\overset{k_6}{\rightleftharpoons}} \text{Pro}_2\text{i} \tag{1f}$$

$$\text{ncRNA} \xrightarrow{k_7} \emptyset \tag{1g}$$

$$\text{mRNA} + \text{ncRNA} \xrightarrow{k_8} \emptyset \tag{1h}$$

The first four reactions are, respectively, transcription from promoter 1 (Pro_1), and translation of the gene for the protein (P), degradation of the mRNA, and degradation of the protein. Reaction (1e) represents the transcription of the non-coding RNA from promoter 2 (Pro_2). Reaction (1f) describes the cooperative binding of n molecules of the protein to promoter 2, which prevents the binding of RNA polymerase to this promoter. Reaction (1g) represents degradation of the ncRNA, while reaction (1h) is a single-step representation of the binding of the non-coding RNA to the mRNA and of the subsequent degradation of the complex [32]. The delays τ_2, τ_4 and τ_6 are the usual synthesis delays encountered in many gene expression models [33–37]. The delay τ_1 represents

5

the time it takes for an RNA polymerase to clear promoter 1, during which time another polymerase cannot bind. Similarly, τ_5 is the promoter clearance time for promoter 2. The delay τ_3 accounts for the time needed for a ribosome to clear its binding site on the mRNA.

The delayed mass-action reactions are to be interpreted as follows, considering the rate of change of the promoter concentration due to reaction (1a) as an example: The instantaneous rate of transcription initiation from promoter 1 is $k_1[\text{Pro}_1]$. This is the pseudo-first-order rate at which promoters enter the transcriptional process, as illustrated in Fig. 1. Promoters that initiate at time t will be cleared at time $t + \tau_1$. The rate at which promoters are cleared of RNA polymerase at time t therefore depends on the rate of initiation at $t - \tau_1$. Thus, at time t, free promoters are removed from the pool at a rate $k_1[\text{Pro}_1](t)$, and returned to that pool at a rate $k_1[\text{Pro}_1](t - \tau_1) \equiv k_1[\text{Pro}_1]_{\tau_1}$, the subscript denoting a delayed quantity.

Applying this reasoning to the full mechanism, we obtain the following delay-differential equations (DDEs) for this model:

$$\frac{d[\text{Pro}_1]_d}{dt} = -k_1[\text{Pro}_1]_d + k_1[\text{Pro}_1]_{d,\tau_1}, \tag{2a}$$

$$\frac{d[\text{mRNA}]_d}{dt} = k_1[\text{Pro}_1]_{d,\tau_2} - k_2[\text{mRNA}]_d$$
$$+ k_2[\text{mRNA}]_{d,\tau_3} - k_3[\text{mRNA}]_d \tag{2b}$$
$$- k_8[\text{mRNA}]_d[\text{ncRNA}]_d,$$

$$\frac{d[\text{P}]_d}{dt} = k_2[\text{mRNA}]_{d,\tau_4} - k_4[\text{P}]_d$$
$$- nk_6[\text{Pro}_2]_d[\text{P}]_d^n + nk_{-6}[\text{Pro}_2\text{i}]_d, \tag{2c}$$

$$\frac{d[\text{Pro}_2]_d}{dt} = -k_5[\text{Pro}_2]_d + k_5[\text{Pro}_2]_{d,\tau_5}$$
$$- k_6[\text{Pro}_2]_d[\text{P}]_d^n + k_{-6}[\text{Pro}_2\text{i}]_d, \tag{2d}$$

$$\frac{d[\text{Pro}_2\text{i}]_d}{dt} = k_6[\text{Pro}_2]_d[\text{P}]_d^n - k_{-6}[\text{Pro}_2\text{i}]_d, \tag{2e}$$

$$\frac{d[\text{ncRNA}]_d}{dt} = k_5[\text{Pro}_2]_{d,\tau_6} - k_7[\text{ncRNA}]_d$$
$$- k_8[\text{mRNA}]_d[\text{ncRNA}]_d. \tag{2f}$$

6

In these equations, the subscript d indicates concentrations in the model with delays. As described above, a subscript τ_i indicates that the corresponding term is evaluated at $t - \tau_i$.

The total amount of each promoter must be conserved. The conservation of promoter 1 is expressed by the following integral equation:

$$[\text{TPro}_1]_d = [\text{Pro}_1]_d(t) + k_1 \int_{t-\tau_1}^{t} [\text{Pro}_1]_d(\theta)\, d\theta, \tag{3}$$

where $[\text{TPro}_1]_d$ is the constant total amount of promoter. Note that $k_1[\text{Pro}_1]_d(\theta)$ is the rate at which promoters were becoming occluded at time $\theta \in [t - \tau_1, t]$. Thus, the integral term in Eq. (3) represents the total amount of promoter that became occluded by RNA polymerase between $t - \tau_1$ and t. Adding the amount of occluded promoter to the amount of free promoter gives the total amount of promoter 1, $[\text{TPro}_1]_d$.

To prove that $[\text{TPro}_1]_d$ is a constant, take a time derivative of Eq. (3):

$$\frac{d[\text{TPro}_1]_d}{dt} = \frac{d[\text{Pro}_1]_d}{dt} + k_1[\text{Pro}_1]_d(t) - k_1[\text{Pro}_1]_d(t - \tau_1).$$

Using Eq. (2a), we find that $d[\text{TPro}_1]_d/dt = 0$, which completes the proof. We can very similarly show that

$$[\text{TPro}_2]_d = [\text{Pro}_2]_d(t) + [\text{Pro}_2\text{i}]_d(t) + k_5 \int_{t-\tau_5}^{t} [\text{Pro}_2]_d(\theta)\, d\theta, \tag{4}$$

the total amount of promoter 2, is a constant of the motion.

At a steady state, when $[\text{Pro}_1]_d$ is constant, Eq. (3) reduces to

$$[\text{TPro}_1]_d = [\text{Pro}_1]_d(1 + k_1\tau_1). \tag{5}$$

Similarly, the steady-state values of $[\text{Pro}_2]_d$ and $[\text{Pro}_2\text{i}]_d$ satisfy, from Eq. (4),

$$[\text{TPro}_2]_d = [\text{Pro}_2]_d(1 + k_5\tau_5) + [\text{Pro}_2\text{i}]_d. \tag{6}$$

The following is therefore a full set of equations for the steady states of this system:

$$k_1[\text{Pro}_1]_d - k_3[\text{mRNA}]_d - k_8[\text{mRNA}]_d[\text{ncRNA}]_d = 0, \tag{7a}$$

$$k_2[\text{mRNA}]_d - k_4[\text{P}]_d = 0, \tag{7b}$$

$$k_5[\text{Pro}_2]_d - k_7[\text{ncRNA}]_d - k_8[\text{mRNA}]_d[\text{ncRNA}]_d = 0, \tag{7c}$$

$$k_6[\text{Pro}_2]_d[\text{P}]_d^n - k_{-6}[\text{Pro}_2\text{i}]_d = 0, \tag{7d}$$

$$[\text{TPro}_1]_d = [\text{Pro}_1]_d(1 + k_1\tau_1), \tag{7e}$$

$$[\text{TPro}_2]_d = [\text{Pro}_2]_d(1 + k_5\tau_5) + [\text{Pro}_2\text{i}]_d. \tag{7f}$$

Note the appearance of the delays τ_1 and τ_5 in Eqs. (7e) and (7f). The steady states of this model thus depend on the promoter-clearance delays due to the appearance of these delays in conservation relations. The steady states are independent of the synthesis delays τ_2, τ_4 and τ_6, as expected. The steady states are also independent of the ribosome-binding-site clearance time τ_3 because the mRNA concentration is not a conserved quantity.

2.2. The model without delays

If we set all of the delays to zero in the mechanism (1) [or, equivalently, in the DDEs (2)], we get the following set of ordinary differential equations:

$$\frac{d[\text{mRNA}]_{nd}}{dt} = k_1[\text{Pro}_1]_{nd} - k_3[\text{mRNA}]_{nd}$$
$$- k_8[\text{mRNA}]_{nd}[\text{ncRNA}]_{nd}, \tag{8a}$$

$$\frac{d[\text{P}]_{nd}}{dt} = k_2[\text{mRNA}]_{nd} - k_4[\text{P}]_{nd}$$
$$- nk_6[\text{Pro}_2]_{nd}[\text{P}]_{nd}^n + nk_{-6}[\text{Pro}_2\text{i}]_{nd}, \tag{8b}$$

$$\frac{d[\text{Pro}_2\text{i}]_{nd}}{dt} = k_6[\text{Pro}_2]_{nd}[\text{P}]_{nd}^n - k_{-6}[\text{Pro}_2\text{i}]_{nd}, \tag{8c}$$

$$\frac{d[\text{ncRNA}]_{nd}}{dt} = k_5[\text{Pro}_2]_{nd} - k_7[\text{ncRNA}]_{nd}$$
$$- k_8[\text{mRNA}]_{nd}[\text{ncRNA}]_{nd}. \tag{8d}$$

The subscript 'nd' indicates quantities in the non-delayed model. Note that in the absence of delays, $[\text{Pro}_1]$ becomes constant. Moreover, the conservation relation (4) reduces to

$$[\text{TPro}_2]_{nd} = [\text{Pro}_2]_{nd} + [\text{Pro}_2\text{i}]_{nd}. \tag{9}$$

The steady-state conditions for this model are obtained straightforwardly from Eqs. (8) and (9):

$$k_1[\text{Pro}_1]_{nd} - k_3[\text{mRNA}]_{nd} - k_8[\text{mRNA}]_{nd}[\text{ncRNA}]_{nd} = 0, \qquad (10\text{a})$$

$$k_2[\text{mRNA}]_{nd} - k_4[\text{P}]_{nd} = 0, \qquad (10\text{b})$$

$$k_5[\text{Pro}_2]_{nd} - k_7[\text{ncRNA}]_{nd} - k_8[\text{mRNA}]_{nd}[\text{ncRNA}]_{nd} = 0, \qquad (10\text{c})$$

$$k_6[\text{Pro}_2]_{nd}[\text{P}]_{nd}^n - k_{-6}[\text{Pro}_2\text{i}]_{nd} = 0, \qquad (10\text{d})$$

$$[\text{TPro}_1]_{nd} = [\text{Pro}_1]_{nd}, \qquad (10\text{e})$$

$$[\text{TPro}_2]_{nd} = [\text{Pro}_2]_{nd} + [\text{Pro}_2\text{i}]_{nd}. \qquad (10\text{f})$$

Equation (10e), which expresses the constancy of $[\text{Pro}_1]$, is included to highlight the parallel structures of Eqs. (7) and (10).

2.3. Parameters

Some of the parameters used here were either directly borrowed from Zhdanov's work [29] or calculated to correspond to the parameters where bistability was observed in his model. Others were estimated as briefly discussed below.

Zhdanov's variables and parameters were scaled so that they represented molecular counts per cell (presumably averaged over many cells, hence the continuous variables). Focusing on bacterial parameters, the number of genome copies per cell varies with growth rate from 1.6 to 4 in *Escherichia coli* [38]. The total amount of the protein-coding promoter (Pro1) was therefore assumed to be 2. The total amount of the ncRNA promoter (Pro2) was assumed to be 10, since multiple copies of an ncRNA sequence can be present in a genome [32].

k_1 and k_5 were chosen to fall within the typical range for transcription initiation by bacterial RNA polymerase given by Record et al. [39]. This assumes that transcription initiation rates for non-coding RNAs are similar to those for coding RNAs.

τ_1 and τ_5 were chosen to be 0.09 min, at the lower end of values for prokaryotes, on the assumption that promoter escape is the rate-limiting process for promoter clearance [21]. At worst, these values of τ_1 and τ_5 will therefore be underestimates.

Table 1: Default parameter values. [t] denotes a value discussed in the text, and [a] represents an assumed value.

Parameter	Value	Reference
Protein expression		
$[\text{TPro}_1]$	2	[t]
k_1	$1.2\,\text{min}^{-1}$	[t]
k_2	$2.3\,\text{min}^{-1}$	[41]
k_3	$0.1\,\text{min}^{-1}$	[29]
τ_1	$0.09\,\text{min}$	[t]
ncRNA expression		
$[\text{TPro}_2]$	10	[t]
k_5	$10\,\text{min}^{-1}$	[t]
k_6	$0.1\,\text{molecule}^{-n}\text{min}^{-1}$	[a]
k_{-6}	$5\,\text{min}^{-1}$	[a]
k_7	$1\,\text{min}^{-1}$	[a]
n	4	[29]
τ_5	$0.09\,\text{min}$	[t]
mRNA-ncRNA complex formation and removal		
k_8	$0.02\,\text{molecule}^{-1}\text{min}^{-1}$	[29]

No value is given for k_4, as this will be used as a control parameter in the bifurcation studies to follow. This rate constant can be varied experimentally given that protein stability can be engineered [40].

3. Bistability

3.1. Geometric argument

We can show that this model has the potential for bistability by a geometric argument. Equation (7e) can be solved analytically for $[\text{Pro}_1]_d$:

$$[\text{Pro}_1]_d = \frac{[\text{TPro}_1]_d}{1 + k_1\tau_1}. \tag{11}$$

Thus, $[\text{Pro}_1]_d$ is a fixed fraction of $[\text{TPro}_1]_d$. Accordingly, in the equations that follow, we leave $[\text{Pro}_1]_d$ as is, with the understanding that we could use Eq. (11) to compute the promoter concentration as needed. We also temporarily drop the d subscripts as there is no possibility of confusion between models here. We then carry out a series of successive eliminations using Eqs. (7a)–(7d) and (7f), resulting in the following equation for the steady-state value of $[\text{P}]$: $f([\text{P}]) = g([\text{P}])$ with

$$f([\text{P}]) = (k_1 k_2 [\text{Pro}_1] - k_3 k_4 [\text{P}]) \left(\frac{1}{k_2} + \frac{k_7}{k_4 k_8 [\text{P}]} \right), \tag{12a}$$

$$g([\text{P}]) = \frac{k_5 [\text{TPro}_2]}{K_6 [\text{P}]^n + 1 + k_5 \tau_5}, \tag{12b}$$

where $K_6 = k_6 / k_{-6}$ is a binding constant. Note that $f([\text{P}]) \to \infty$ as $[\text{P}] \to 0$ and that

$$\frac{df}{d[\text{P}]} = -\frac{k_3 k_4}{k_2} - \frac{k_1 k_2 k_7 [\text{Pro}_1]}{k_4 k_8 [\text{P}]^2} < 0 \tag{13}$$

for $[\text{P}] > 0$. $f([\text{P}]) = 0$ intersects the $[\text{P}]$ axis at

$$[\text{P}]_0 = \frac{k_1 k_2 [\text{Pro}_1]}{k_3 k_4}. \tag{14}$$

$g([\text{P}])$ on the other hand is a strictly decreasing Hill function with a maximum value

$$g_{\max} = \frac{k_5 [\text{TPro}_2]}{1 + k_5 \tau_5}, \tag{15}$$

and reaches half this maximum value at

$$[\text{P}]_{1/2} = \left(\frac{1 + k_5 \tau_5}{K_6} \right)^{1/n}. \tag{16}$$

This combination of geometric properties of f and g allows for one, two (at saddle-node bifurcations) or three steady states. Figure 2 shows a typical case with three intersections. If $f([\text{P}])$ decreases too fast, there will only be one intersection with the initial plateau of $g([\text{P}])$ at small $[\text{P}]$. On the other hand, if $f([\text{P}])$ decreases very slowly, there may only be one intersection with the asymptotic plateau at large values of $[\text{P}]$.

In the case that there are three intersections, we can obtain some rough estimates for the stable (outer) steady states as follows: The first intersection
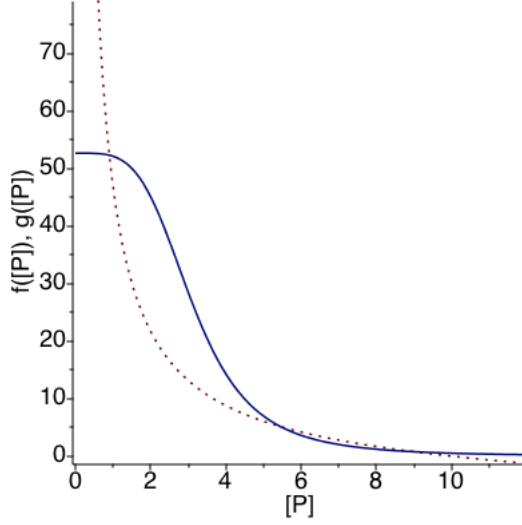
11

Figure 2: $f([P])$ (Eq. (12a), red, dotted) and $g([P])$ (Eq. (12b), blue, solid) for the parameters of Table 1 with $k_4 = 5\,\mathrm{min}^{-1}$. Steady states of the model occur at intersections of $f([P])$ and $g([P])$.

tends to occur in the plateau where $g([P]) \approx g_{\max}$. This occurs at small $[P]$ where

$$f([P]) \approx \frac{k_1 k_2 k_7 [\mathrm{Pro}_1]}{k_4 k_8 [P]}. \tag{17}$$

Thus, the low-$[P]$ steady state occurs near

$$[P]_1 \approx \frac{k_1 k_2 k_7 [\mathrm{Pro}_1](1 + k_5 \tau_5)}{k_4 k_5 k_8 [\mathrm{TPro}_2]}, \tag{18}$$

numbering the three steady states from left to right. Because $g([P])$ decreases very quickly for $[P] > [P]_{1/2}$, it has a small value where the high-$[P]$ steady state occurs. Thus, $[P]_3 \lesssim [P]_0$. These are very rough estimates, but they will be useful later for understanding the effects of some of the parameters on the bifurcation structure.

Note that these arguments still hold if we set $\tau_1 = \tau_5 = 0$, i.e. the model without delays will also display bistability, as expected given the close relationship of this model to Zhdanov's [29].
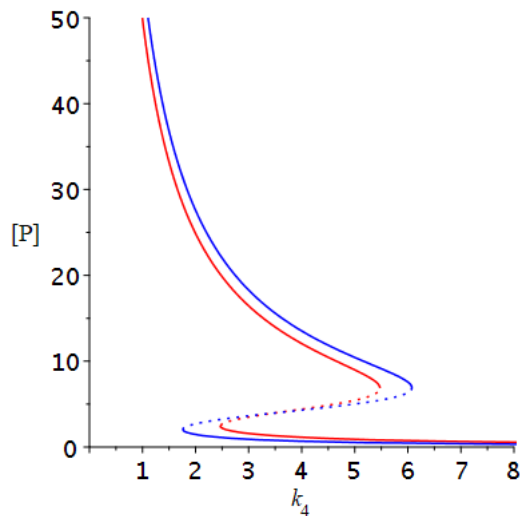
Figure 3: Steady-state solutions for the models with binding-site clearance delays (red) and without these delays (blue) for the parameters of Table 1. Solid segments indicate stable steady states, and dotted segments are branches of unstable steady states.

3.2. Numerical comparison of models with and without delays

Using the parameters of Table 1, we computed bifurcation diagrams for the models with and without delays by solving Eqs. (7) and (10), respectively. The results are shown in Fig. 3. These models display bistability, just as Zhdanov's model does [29]. However, the range of bistability for the model without binding-site clearance delays is wider than for the full model. In other words, leaving out the clearance-site delays, which are small and might be thought to be negligible, exaggerates the tendency of this system toward bistability. Moreover, it should be noted that the values of τ_1 and τ_5 chosen are at the low end of the observed range [20–22]. If we choose a larger value for τ_1, the steady-state curve shifts dramatically to the left [Fig. 4(a)], i.e. the quantitative differences seen in Fig. 3 are amplified when τ_1 increases. However, bistability is not typically lost by increasing τ_1. To understand this, recall that increasing τ_1 decreases $[\text{Pro}_1]$ [Eq. (11)]. The approximate equations for the two stable steady states, Eqs.

(14) and (18), both depend on the combination of parameters

$$\phi = k_1 k_2 [\text{Pro}_1]/k_4. \tag{19}$$

Thus, if we decrease $[\text{Pro}_1]$, a bifurcation diagram against k_4 simply shifts to smaller values of the control parameter. Having said that, the range over which bistability occurs may decrease to the point where it is not relevant experimentally. Similar comments could be made for other combinations of parameters appearing in Eq. (19).

The steady-state curve is even more sensitive to τ_5, and bistability disappears completely for sufficiently large values of this clearance delay [Fig. 4(b)], completely altering the dynamics of the gene circuit. Thus the clearance delays τ_1 and τ_5 have quite different effects, despite the similar roles they play in the respective transcription steps 1a and 1e. Note that the largest value of τ_5 considered in Fig. 4(b), 3 min, is well within the experimentally observed range in prokaryotes [11, 20–22]. Thus, evolution can tune the DNA sequence near the promoter, and hence the promoter clearance delay, to favor either a single steady state or bistability, according to the functional requirements of a gene circuit.

Given that gene copy numbers change as the cell replicates its DNA, we briefly consider what happens when we change $[\text{TPro}_1]$ and $[\text{TPro}_2]$. From Eqs. (11) and (18), it is clear that the low-$[P]$ steady state ($[P]_1$) depends on the ratio of $[\text{TPro}_1]$ to $[\text{TPro}_2]$. Thus, replicating the entire genome does not affect this steady state. On the other hand, Eqs. (11) and (14) together imply that the high-$[P]$ branch of steady states ($[P]_3 \sim [P]_0$), should depend roughly linearly on $[\text{TPro}_1]$, keeping other parameters constant. If we define the number of genome copies c such that

$$([\text{TPro}_1], [\text{TPro}_2]) = c(1, 5), \tag{20}$$

which maintains the ratio of the two promoters in Table 1, and vary c, we obtain the bifurcation diagram shown in Fig. 5. As suggested by the foregoing analysis, the lower branch of steady states is essentially independent of c, while the upper branch increases roughly linearly with c away from the saddle-node point.
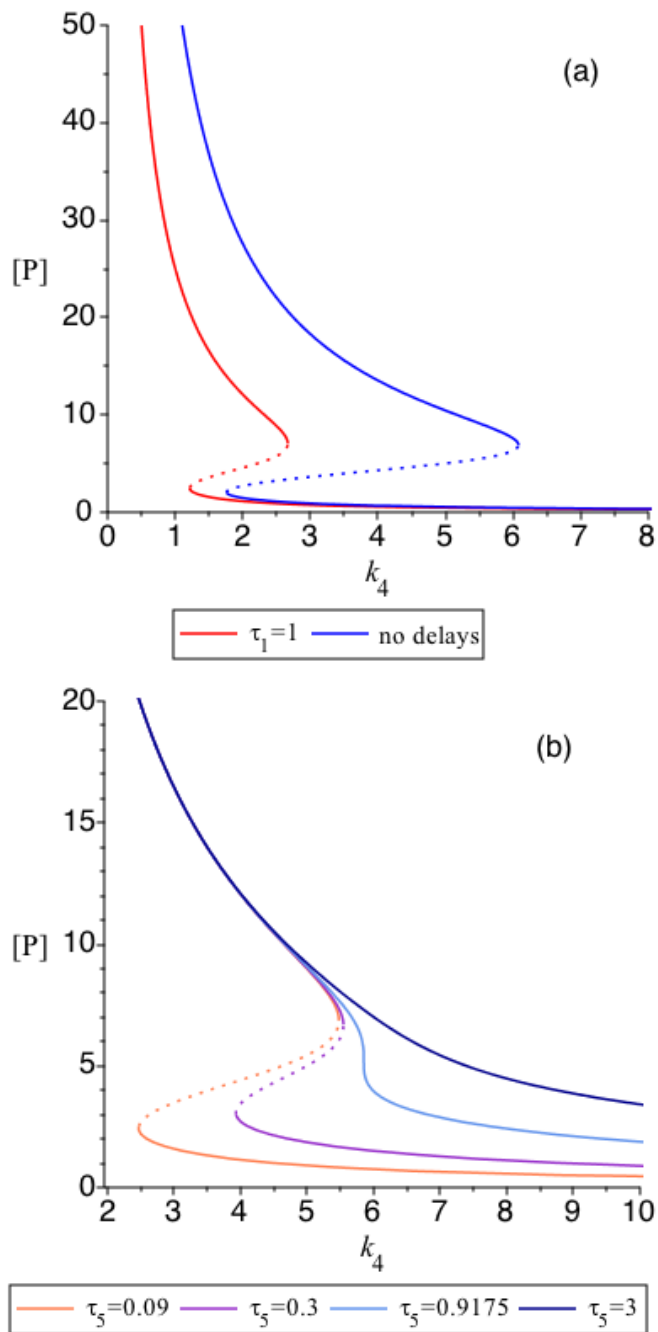
14

Figure 4: (a) Steady-state solutions for the models with (red) and without (blue) binding-site clearance delays for the parameters of Table 1 except $\tau_1 = 1\,\text{min}$. (b) Steady-state solutions of the model with delays for the parameters of Table 1, but at different values of τ_5.
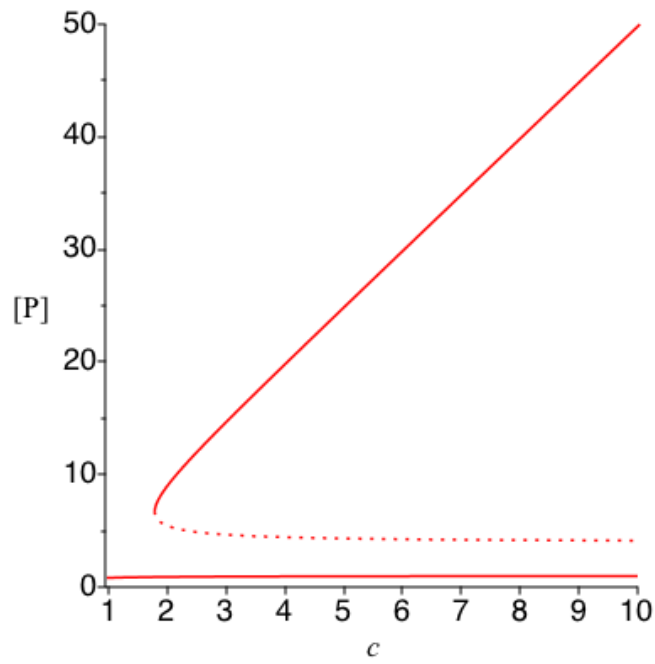
Figure 5: Effect of the number of copies of the genome on the steady states of the model. The copy number c is defined by Eq. (20). Other parameters are set as in Table 1 with $k_4 = 5\,\mathrm{min}^{-1}$.

4. Relationship between models with and without delays

Let us compare the steady-state equations of the two models. The first four equations of sets (7) and (10), the equations obtained directly from the rate equations, are identical. From the point of view of their steady-state structures, the difference between the two models occurs in the conservation relations for the promoters, Eqs. (7e)–(7f) on the one hand, or (10e)–(10f) on the other. In order to bring the two models into agreement, it is only necessary to arrange for them to have the same solutions for the free promoter concentrations $[\mathrm{Pro}_1]$ and $[\mathrm{Pro}_2]$. Then $[\mathrm{P}]$ will have the same value in both models because Eqs. (7a)–(7c) and (10a)–(10c) are identical.

Combining Eqs. (10e) and (11), we find that $[\mathrm{Pro}_1]_d = [\mathrm{Pro}_1]_{nd}$ if

$$[\mathrm{TPro}_1]_{nd} = \frac{[\mathrm{TPro}_1]_d}{1 + k_1 \tau_1}. \tag{21}$$

This relationship corrects for the reduction in the concentration of available Pro_1 in the model without delays due to the occlusion of the binding site during a time τ_1.

The situation is more complex at promoter 2 due to the equilibrium (1f). From Eq. (7d) or the identical (10d), we get

$$[\mathrm{Pro}_2\mathrm{i}] = K_6 [\mathrm{Pro}_2][\mathrm{P}]^n, \tag{22}$$

with implied subscripts d or nd according to the model. We can then substitute this expression into (7f) and (10f) and solve for the promoter concentrations:

$$[\mathrm{Pro}_2]_d = \frac{[\mathrm{TPro}_2]_d}{1 + k_5 \tau_5 + K_6 [\mathrm{P}]^n}, \tag{23a}$$

$$[\mathrm{Pro}_2]_{nd} = \frac{[\mathrm{TPro}_2]_{nd}}{1 + K_6 [\mathrm{P}]^n}. \tag{23b}$$

To bring Eqs. (23a) and (23b) into a common form, divide the numerator and denominator of (23a) by $1 + k_5 \tau_5$:

$$[\mathrm{Pro}_2]_d = \frac{\dfrac{[\mathrm{TPro}_2]_d}{1 + k_5 \tau_5}}{1 + \dfrac{K_6 [\mathrm{P}]^n}{(1 + k_5 \tau_5)}}. \tag{24}$$

17

Comparing Eqs. (23b) and (24), we see that the two *cannot* be brought into correspondence if the two models are to use the same value of the binding constant K_6. Labeling the latter quantity with subscripts d and nd as appropriate, equivalence of the two models requires

$$[\text{TPro}_2]_{nd} = \frac{[\text{TPro}_2]_d}{1 + k_5 \tau_5}, \tag{25a}$$

$$K_{6,nd} = \frac{K_{6,d}}{1 + k_5 \tau_5}. \tag{25b}$$

Equations (11) and (25a) are simple rescalings of promoter concentrations. One might be tempted to dismiss such rescalings as straightforward connections between total and free promoter concentrations. However, the binding constant K_6 is an experimentally measurable quantity. An ad hoc adjustment of this constant (or, equivalently, of one of the rate constants k_6 or k_{-6}), which would be required in a model without clearance delays, lacks any reasonable justification. In general, ad hoc adjustments of kinetic constants are considered poor practice in reaction network modeling [42]. Note that for the parameters chosen here, $1 + k_1 \tau_1 = 1.1$ and $1 + k_5 \tau_5 = 1.9$, using promoter clearance times at the low end of the experimentally observed range and initiation rate constants within the range observed in *E. coli*. Arguably, a 10% correction in $[\text{Pro}_1]$ is within the range where this effect might be ignored given the well-known uncertainties in gene expression modeling. It is more difficult to argue that nearly two-fold corrections not only in an effective promoter concentration but also in a physico-chemical parameter are negligible.

Specializing Eq. (22) to the model without delays and using Eq. (25b) to express $K_{6,nd}$ in terms of the true binding constant $K_6 \equiv K_{6,d}$, we get

$$[\text{Pro}_2\text{i}]_{nd} = \frac{K_6 [\text{Pro}_2][\text{P}]^n}{1 + k_5 \tau_5}. \tag{26}$$

If we have performed the parameter transformations discussed above, then the steady-state values of $[\text{Pro}_2]$ and $[\text{P}]$ are the same in the two models, hence the lack of subscripts on these quantities. Comparing the latter equation to Eq. (22) specialized to the delay case establishes a relationship between the

Pro₂i concentrations in the two models:

$$[\text{Pro}_2\text{i}]_{nd} = \frac{[\text{Pro}_2\text{i}]_d}{1 + k_5\tau_5}. \tag{27}$$

The cost of adjusting the value of $K_{6,nd}$ in order for the model without delays to match protein and RNA levels predicted by the model with clearance delays is therefore that the concentration of $[\text{Pro}_2\text{i}]$ is rescaled in the model without delays. To put it another way, if the model without delays were used to analyze experimental data, fitting an experimental bifurcation curve would result in a mismatch between true repressed promoter concentrations and model predictions for $[\text{Pro}_2\text{i}]$. Figure 6 illustrates this discrepancy.

The analysis of this section has emphasized bringing the two models into correspondence, but there are some subtle differences, including an important difference with respect to mRNA levels. As noted earlier, the steady-state equations (7) do not depend on the ribosome-binding-site clearance delay τ_3. Correspondingly, the free mRNA levels in the two models can be made identical as shown above. However, the model with delays has an implicit "protected" pool of mRNAs on which translation has been initiated, but whose ribosome binding sites have not yet been exposed. These mRNAs are protected from degradation through reaction (1c), which only acts on mRNAs with a cleared ribosome binding site. This is not a model artifact but a well known biochemical phenomenon [16, 19, 43] due to the preponderance of $5' \rightarrow 3'$ exonucleases in cellular mRNA decay processes.

The total amount of mRNA in the model with delays can be computed as follows: Imagine that at time $t = t_0$, all RNA polymerases are halted so that no further transcription processes can either be initiated or completed. At the same time, we inhibit all mRNA degradation processes as well as translation initiation. However, we allow initiated translation processes to "run off". (There is a rough experimental counterpart to this gedanken experiment [16].) Equation (2b) therefore becomes

$$\frac{d[\text{mRNA}]_d}{dt} = \kappa_2(t - \tau_3)[\text{mRNA}]_{d,\tau_3}, \tag{28}$$
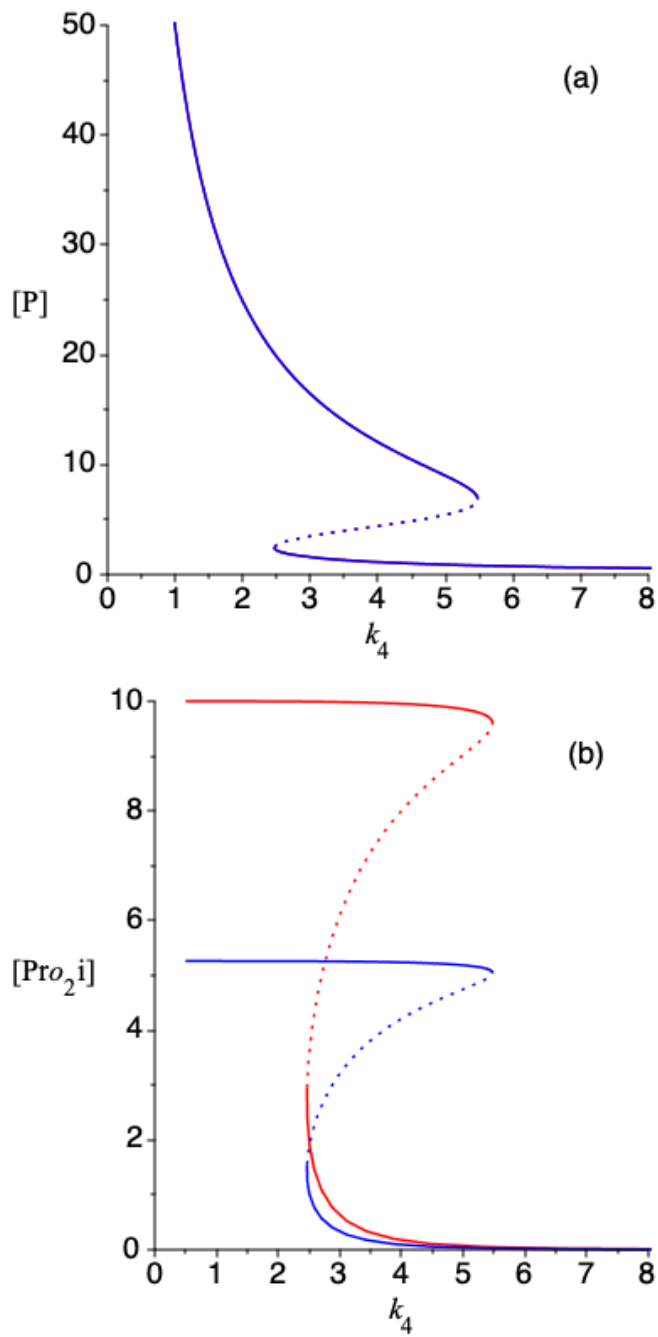
19

Figure 6: Bifurcation curves for the models with and without delays using the parameters of Table 1 and the adjustments of Eqs. (21), (25a) and (25b). In both panels the solutions from the model with delays are in red, and the solutions from the model without delays are in blue. In panel (a), the concentrations of P are identical at every value of k_4. The same is true of all of the other concentrations in the model, except for [Pro$_2$i], illustrated in panel (b).

with

$$\kappa_2(\theta) = \begin{cases} k_2 & \text{if } \theta \leq t_0, \\ 0 & \text{if } \theta > t_0. \end{cases} \qquad (29)$$

The solution of this equation is

$$[\text{mRNA}]_d(t) = [\text{mRNA}]_d(t_0)$$

$$+ k_2 \int_{t_0}^{\min(t, t_0 + \tau_3)} [\text{mRNA}]_d(\theta - \tau_3) \, d\theta \quad (30)$$

for any $t > t_0$. The asymptotic value is the total amount of mRNA at time t_0. In a steady state, the latter reduces to

$$[\text{mRNA}]_{\text{total}} = [\text{mRNA}]_d(1 + k_2\tau_3). \qquad (31)$$

Thus, the total pool of mRNA is greater in the model with delays by a factor of $1 + k_2\tau_3$ than in the model without delays.

5. Discussion and conclusions

We analyzed a model with both expression (transcription and translation) delays and binding-site clearance delays, and compared the bifurcation diagram of this model to that of an equivalent model without delays. We found that the binding-site clearance delays can have a significant effect on the bifurcation diagram. Larger, but still physiologically realistic values of the delays can completely abolish bistability in this model. Thus, binding-site clearance delays, which are typically neglected, can qualitatively change the dynamics of a gene expression model. The same issue would arise in comparing a model such as (1) to one with only expression delays given that the steady states depend on the clearance delays, but not on the expression delays. We are currently also studying the effects of clearance delays in a model with an Andronov-Hopf bifurcation [44].

In many cases, gene expression models are qualitative descriptions of imperfectly understood systems. In these cases, a certain latitude in the inclusion of

21

detailed promoter kinetics is certainly defensible. And of course, highly simplified models such as (1) involve a number of approximations of their own. However, it is increasingly possible to write down models for which many of the parameters are either known directly from experiments, or can be estimated with reasonable precision. In these cases, it is worthwhile to consider carefully the effects of any approximations, such as leaving out binding-site clearance delays.

Even in the context of this simple model, we encountered three classes of clearance delays:

1. Harmless clearance delays that do not affect the steady states of the model [45]. Clearance from non-conserved species such as the ribosome binding site falls into this category.

2. Delays that can be removed by a simple rescaling of a conserved quantity. In gene expression models, transcription from a constitutive promoter such as Pro_1 in this model would generally be removable in this sense.

3. Delays whose removal requires alteration of kinetic parameters. This will be an issue for transcription from a promoter whose activity is controlled by the binding of a regulatory factor.

Of course, fixed delays are an approximation to distributed delays, but given the issues highlighted here, fixed delays are probably preferable to not including binding-site clearance effects at all. Equally, we could avoid clearance delays altogether by including a very detailed model of events from the beginning of initiation until the completion of binding-site clearance. In many cases though, it may be difficult to parameterize such a model, and this would certainly greatly increase model complexity without necessarily adding much to our understanding.

Model parameters are often fit from experimental data. Given that the projections of the steady-state solutions into the $([Pro_1], [mRNA], [P], [Pro_2], [ncRNA])$ positive orthant are identical, experimental data from a system with the kinetics (1) could equally well be fit to either model provided we do not measure

22

[Pro$_2$i]. Suppose that appropriate steady-state experimental data were used to estimate the parameters of the model without delays. The result would be an underestimate of [TPro$_1$] by a factor of $1 + k_1\tau_1$, and underestimates of [TPro$_2$] and K_6, both by a factor of $1 + k_5\tau_5$. It would then become difficult to reconcile parameter estimates from fitting the model without delays to direct measurements of these quantities. This may be seen as an unfair criticism of the model without delays since steady-state experiments alone would not allow the identification of the delays. However, it would be possible to use typical values or, better yet, a range of typical values, to determine how the clearance delays affect the estimates of the other model parameters.

The model (1) is sufficiently simple that we were able to carry out a full analysis to discover the relationship between the parameters of the two models leading to a steady-state isomorphism in the ([Pro$_1$], [mRNA], [P], [Pro$_2$], [ncRNA]) positive orthant. However, a similar depth of analysis may be difficult or impossible in more complex models. The extent to which the results of simulations from estimated parameters would be affected by the neglect of the binding-site clearance delays would therefore typically be unknown. Even knowing which parameters need to be adjusted to account for neglect of the clearance delays may be difficult. It was certainly not obvious a priori that matching the two models would require an adjustment in K_6. Consequently, our recommendation would be to include these delays in any modeling work where either good parameter estimates are available for most of the model parameters, or where sufficient experimental data of reasonable quality are available to fit the identifiable parameters of a detailed model such as (1). Even if it becomes necessary to experiment with different values of the binding-site clearance delays, at least the sensitivity of the results to the values of these delays will then become known.

There is one additional dimension to consider, which is that differential equation models, while valuable for exploring the phenomenology of a gene expression system, are best thought of as ensemble models since stochastic dynamics dominates gene expression in a single cell. Delays can be incorporated into stochastic models [7, 46–48], and in fact it is easier to treat distributed de-

23

lays in delay-stochastic models (at least from a simulation point of view) than in differential-equation models [7]. Since bistable systems display stochastic switching between the two steady states [29, 49], given the effects on the bifurcation diagrams observed here, models with and without binding-site clearance delays would presumably display different switching kinetics. It is not clear at this time whether the adjustments described here would correct the stochastic switching kinetics since they necessarily require adjustments to some of the kinetic constants for regulated genes (e.g. k_6 or k_{-6} in this model). This is clearly an important area for future investigation.

It would also be interesting to study a stochastic model incorporating cell growth and DNA replication. The variables and parameters in the model studied here have been scaled (as in Zhdanov's work [29]) to give molecular counts per cell. In order to study a model with cell division, we would need to use conventional volumic concentrations and associated rate constants. The scaling parameter c used to generate Fig. 5 could then be reinterpreted as the number of genome copies per unit volume. An increase in volume without DNA synthesis would slide the system to the left in Fig. 5. Conversely, DNA synthesis at a rate exceeding the rate of volume increase would move the system to the right in the bifurcation diagram. The rate of stochastic switching from the upper to the lower branch would increase when c is small, i.e. when the cell has reached its maximum volume prior to undertaking DNA synthesis, due to the decreased distance between the upper stable and middle unstable branches of steady states. On the other hand, the rate of switching from the lower branch to the upper branch would be relatively constant throughout the cell cycle since neither the lower stable nor the middle unstable steady state depends much on c, provided of course c doesn't slip below the value where the saddle-node bifurcation occurs. This is a highly simplified account of the likely stochastic dynamics given that the stochastic dynamics is generally not fully captured by the deterministic bifurcation diagram [49–52]. It would be interesting to see what dynamics would emerge from such a model.

24

Author contributions

E. A. M. Trofimenkoff: Methodology, Investigation, Formal analysis, Writing – Original draft. M. R. Roussel: Conceptualization, Validation, Formal analysis, Writing – Review & editing, Supervision, Funding acquisition

Declaration of interest

All authors declare that they have no competing interest.

Acknowledgments

References

[1] C. T. MacDonald, J. H. Gibbs, A. C. Pipkin, Kinetics of biopolymerization on nucleic acid templates, Biopolymers 6 (1968) 1–25. doi:10.1002/bip.1968.360060102.

[2] G. Lakatos, T. Chou, Totally asymmetric exclusion process with particles of arbitrary size, J. Phys. A 36 (2003) 2027–2041. doi:10.1088/0305-4470/36/8/302.

[3] L. B. Shaw, R. K. P. Zia, K. H. Lee, Totally asymmetric exclusion process with extended objects: A model for protein synthesis, Phys. Rev. E 68 (2003) 021910. doi:10.1103/PhysRevE.68.021910.

[4] A. Garai, D. Chowdhury, D. Chowdhury, T. V. Ramakrishnan, Stochastic kinetics of ribosomes: Single motor properties and collective behavior, Phys. Rev. E 80 (2009) 011908. doi:10.1103/PhysRevE.80.011908.

[5] Y. Ohta, T. Kodama, S. Ihara, Cellular-automaton model of the cooperative dynamics of RNA polymerase II during transcription in human cells, Phys. Rev. E 84 (2011) 041922. doi:10.1103/PhysRevE.84.041922.

[6] K. Dao Duc, Z. H. Saleem, Y. S. Song, Theoretical analysis of the distribution of isolated particles in totally asymmetric exclusion processes: Application to mRNA translation rate estimation, Phys. Rev. E 97 (2018) 012106. doi:10.1103/PhysRevE.97.012106.

[7] M. R. Roussel, R. Zhu, Validation of an algorithm for delay stochastic simulation of transcription and translation in prokaryotic gene expression, Phys. Biol. 3 (2006) 274–284. doi:10.1088/1478-3975/3/4/005.

[8] A. Kremling, Comment on mathematical models which describe transcription and calculate the relationship between mrna and protein expression ratio, Biotech. Bioeng. 96 (2007) 815–819. doi:10.1002/bit.21065.

[9] X. chuan Xue, F. Liu, Z. can Ou-Yang, A kinetic model of transcription initiation by RNA polymerase, J. Mol. Biol. 378 (2008) 520–529. doi:10.1016/j.jmb.2008.03.008.

[10] J. Mäkelä, J. Lloyd-Price, O. Yli-Harja, A. S. Ribeiro, Stochastic sequence-level model of coupled transcription and translation in prokaryotes, BMC Bioinformatics 12 (2011) 121. doi:10.1186/1471-2105-12-121.

[11] J. Lloyd-Price, S. Startceva, V. Kandavalli, J. G. Chandraseelan, N. Goncalves, S. M. D. Oliveira, A. Häkkinen, A. S. Ribeiro, Dissecting the stochastic transcription initiation process in live *Escherichia coli*, DNA Res. 23 (2016) 203–214. doi:10.1093/dnares/dsw009.

[12] I. Belgacem, S. Casagranda, E. Grac, D. Ropers, J.-L. Gouzé, Reduction and stability analysis of a transcription-translation model of rna polymerase, Bull. Math. Biol. 80 (2018) 294–318. doi:10.1007/s11538-017-0372-4.

[13] J.-F. Lemay, F. Bachand, Fail-safe transcription termination: Because one is never enough, RNA Biol. 12 (2015) 927–932. doi:10.1080/15476286.2015.1073433.

[14] M. R. Roussel, The use of delay differential equations in chemical kinetics, J. Phys. Chem. 100 (1996) 8323–8330. doi:10.1021/jp9600672.

[15] M. R. Roussel, A delayed mass-action model for the transcriptional control of Hmp, an NO detoxifying enzyme, by the iron-sulfur protein FNR, in: G. Valmorbida, A. Seuret, I. Boussaada, R. Sipahi (Eds.), Delays and Interconnections: Methodology, Algorithms and Applications, Vol. 10 of Advances in Delays and Dynamics, Springer, Cham, 2019, pp. 215–230. doi:10.1007/978-3-030-11554-8_14.

[16] D. Kennell, V. Talkad, Messenger RNA potential and the delay before exponential decay of messages, J. Mol. Biol. 104 (1976) 285–298. doi:10.1016/0022-2836(76)90014-0.

[17] O. Yarchuk, N. Jacques, J. Guillerez, M. Dreyfus, Interdependence of translation, transcription and mRNA degradation in the *lacZ* gene, J. Mol. Biol. 226 (1992) 581–596.

[18] H. Bremer, P. Dennis, M. Ehrenberg, Free RNA polymerase and modeling global transcription in *Escherichia coli*, Biochimie 85 (2003) 597–609. doi:10.1016/S0300-9084(03)00105-6.

[19] M. Eriksen, K. Sneppen, S. Pedersen, Occlusion of the ribosome binding site connects the translational initiation frequency, mrna stability and premature transcription termination, Front. Microbiol. 8 (2017). doi:10.3389/fmicb.2017.00362.

[20] R. Lutz, T. Lozinski, T. Ellinger, H. Bujard, Dissecting the functional program of *Escherichia coli* promoters: The combined mode of action of Lac repressor and AraC activator, Nucleic Acids Res. 29 (2001) 3873–3881. doi:10.1093/nar/29.18.3873.

[21] L. M. Hsu, Promoter clearance and escape in prokaryotes, Biochim. Biophys. Acta 1577 (2002) 191–207. doi:10.1016/S0167-4781(02)00452-9.

[22] N.-N. Aye-Han, L. M. Hsu, Initial transcribed sequence and template conformation affect the rate and RNA polymerase partitioning during promoter escape (unpublished).

[23] J. F. Kugel, J. A. Goodrich, A kinetic model for the early steps of RNA synthesis by human RNA polymerase II, J. Biol. Chem. 275 (2000) 40483–40491. doi:10.1074/jbc.M006401200.

[24] X. Darzacq, Y. Shav-Tal, V. de Turris, Y. Brody, S. M. Shenoy, R. D. Phair, R. H. Singer, *In vivo* dynamics of RNA polymerase II transcription, Nat. Struct. Mol. Biol. 14 (2007) 796–806. doi:10.1038/nsmb1280.

[25] R. Zhu, D. Salahub, Delay stochastic simulation of single-gene expression reveals a detailed relationship between protein noise and mean abundance, FEBS Lett. 582 (2008) 2905–2910. doi:10.1016/j.febslet.2008.07.028.

[26] I. Potapov, J. Lloyd-Price, O. Yli-Harja, A. S. Ribeiro, Dynamics of a genetic toggle switch at the nucleotide and codon levels, Phys. Rev. E 84 (2011) 031903, errata: Phys Rev E 84:069903, DOI 10.1103/PhysRevE.84.069903. doi:10.1103/PhysRevE.84.031903.

[27] M. R. Roussel, R. Zhu, Stochastic kinetics description of a simple transcription model, Bull. Math. Biol. 68 (2006) 1681–1713. doi:10.1007/s11538-005-9048-6.

[28] A. S. Ribeiro, O.-P. Smolander, T. Rajala, A. Häkkinen, O. Yli-Harja, Delayed stochastic model of transcription at the single nucleotide level, J. Comput. Biol. 16 (2009) 539–553. doi:10.1089/cmb.2008.0153.

[29] V. P. Zhdanov, Bistability in gene transcription: Interplay of messenger RNA, protein, and nonprotein coding RNA, BioSystems 95 (2009) 75–81. doi:10.1016/j.biosystems.2008.07.002.

[30] J. Shen, Z. Liu, W. Zheng, F. Xu, L. Chen, Oscillatory dynamics in a simple gene regulatory network mediated by small RNAs, Physica A 388 (2009) 2995–3000. doi:10.1016/j.physa.2009.03.032.

[31] S. Nikolov, J. V. Gonzalez, M. Nenov, O. Wolkenhauer, Dynamics of a miRNA model with two delays, Biotechnol. Biotechnol. Equip. 26 (2012) 3315–3320. doi:10.5504/BBEQ.2012.0067.

[32] L. S. Waters, G. Storz, Regulatory RNAs in bacteria, Cell 136 (2009) 615–628. doi:10.1016/j.cell.2009.01.043.

[33] R. D. Bliss, Analysis of the dynamic behavior of the tryptophan operon of *Escherichia coli*: The functional significance of feedback inhibition, Ph.D. thesis, University of California Riverside (1979).

[34] F. Buchholtz, F. W. Schneider, Computer simulation of T3/T7 phage infection using lag times, Biophys. Chem. 26 (1987) 171–179. doi:10.1016/0301-4622(87)80020-0.

[35] J. M. Mahaffy, Genetic control models with diffusion and delays, Math. Biosci. 90 (1988) 519–533. doi:10.1016/0025-5564(88)90081-8.

[36] J. Lewis, Autoinhibition with transcriptional delay: A simple mechanism for the zebrafish somitogenesis oscillator, Curr. Biol. 13 (2003) 1398–1408. doi:10.1016/S0960-9822(03)00534-7.

[37] N. A. M. Monk, Oscillatory expression of Hes1, p53, and NF-κB driven by transcriptional time delays, Curr. Biol. 13 (2003) 1409–1413. doi:10.1016/S0960-9822(03)00494-9.

[38] H. Bremer, P. P. Dennis, Modulation of chemical composition and other parameters of the cell at different exponential growth rates, Ecosal Plus (2013). doi:10.1128/ecosal.5.2.3.

[39] M. T. Record, Jr., W. S. Reznikoff, M. L. Craig, K. L. McQuade, P. J. Schlax, *Escherichia coli* RNA polymerase (Eσ^{70}), promoters, and the kinetics of the steps of transcription initiation, in: F. C. Neidhardt (Ed.),

Escherichia coli and *Salmonella*: Cellular and Molecular Biology, 2nd Edition, Vol. 2, ASM Press, Washington, 1996, pp. 792–820.

[40] R. Kazlauskas, Engineering more stable proteins, Chem. Soc. Rev. 47 (2018) 9026–9045. doi:10.1039/c8cs00014j.

[41] B. Schwanhäusser, D. Busse, N. Li, G. Dittmar, J. Schuchhardt, JanaWolf, W. Chen, M. Selbach, Global quantification of mammalian gene expression control, Nature 473 (2011) 337–342. doi:10.1038/nature10098.

[42] V. S. Engleman, Detailed approach to kinetic mechanisms in complex systems, J. Phys. Chem. 81 (1977) 2320–2322. doi:10.1021/j100540a004.

[43] H. Chen, K. Shiroguchi, H. Ge, X. S. Xie, Genome-wide study of mRNA degradation and transcript elongation in *Escherichia coli*, Mol. Syst. Biol. 11 (2015) 781, errata: Mol Syst Biol 11:808, DOI 10.15252/msb.20159000. doi:10.15252/msb.20145794.

[44] H. U. Ünal, M. R. Roussel, I. Boussaada, S. I. Niculescu, Insights from a qualitative analysis of a gene expression model with delays, in: 24th International Symposium on Mathematical Theory of Networks and Systems, in review.

[45] R. D. Driver, Some harmless delays, in: K. Schmitt (Ed.), Delay and Functional Differential Equations and Their Applications, Academic, New York, 1972, pp. 103–119.

[46] M. A. Gibson, J. Bruck, Efficient exact stochastic simulation of chemical systems with many species and many channels, J. Phys. Chem. A 104 (2000) 1876–1889. doi:10.1021/jp993732q.

[47] D. Bratsun, D. Volfson, L. S. Tsimring, J. Hasty, Delay-induced stochastic oscillations in gene regulation, Proc. Natl. Acad. Sci. U.S.A. 102 (2005) 14593–14598. doi:10.1073/pnas.0503858102.

[48] M. Barrio, K. Burrage, A. Leier, T. Tian, Oscillatory regulation of Hes1: Discrete stochastic delay modelling and simulation, PLoS Comput. Biol. 2 (2006) e117. doi:10.1371/journal.pcbi.0020117.

[49] T. B. Kepler, T. C. Elston, Stochasticity in transcriptional regulation: Origins, consequences, and mathematical representations, Biophys. J. 81 (2001) 3116–3136. doi:10.1016/S0006-3495(01)75949-8.

[50] A. Lipshtat, A. Loinger, N. Q. Balaban, O. Biham, Genetic toggle switch without cooperative binding, Phys. Rev. Lett. 96 (2006) 188101.

[51] L. M. Bishop, H. Qian, Stochastic bistability and bifurcation in a mesoscopic signaling system with autocatalytic kinase, Biophys. J. 98 (2010) 1–11. doi:10.1016/j.bpj.2009.09.055.

[52] T.-L. To, N. Maheshri, Noise can induce bimodality in positive transcriptional feedback loops without bistability, Science 327 (2010) 1142–1145. doi:10.1126/science.1178962.